

Received March 10, 2021, accepted March 22, 2021, date of publication March 29, 2021, date of current version April 6, 2021.

Digital Object Identifier 10.1109/ACCESS.2021.3069144

# Study of the Complex Permittivity of a Polyurethane Matrix Modified by Nanoparticles

JOZEF KÚDELČÍK<sup>1</sup>, ŠTEFAN HARDOŇ<sup>1</sup>, PETER HOCKICKO<sup>1</sup>, MÁRIA KÚDELČÍKOVÁ<sup>2</sup>,  
JAROSLAV HORNAK<sup>3</sup>, (Member, IEEE), PAVEL PROSR<sup>3</sup>, (Member, IEEE),  
AND PAVEL TRNKA<sup>3</sup>, (Senior Member, IEEE)

<sup>1</sup>Department of Physics, Faculty of Electrical Engineering and Information Technology, University of Žilina, 010 26 Žilina, Slovakia

<sup>2</sup>Department of Structural Mechanics and Applied Mathematics, Faculty of Civil Engineering, University of Žilina, 010 26 Žilina, Slovakia

<sup>3</sup>Department of Technologies and Measurement, Faculty of Electrical Engineering, University of West Bohemia at Pilsen, 301 00 Plzeň, Czech Republic

Corresponding author: Jozef Kúdelčík (jozef.kudelcik@feit.uniza.sk)

This work was supported in part by the Visegrad Fund through the Visegrad Scholarship Program under Grant 52010598 and Strategic Grant 22010345, in part by the Uniza under Grant 7965, and in part by the Student Grant Agency of the University of West Bohemia in Pilsen (Materials, Technologies and Diagnostics in Electrical Engineering) under Grant SGS-2021-003.

**ABSTRACT** This study presents the influence of various types of nanoparticle (NP) fillers incorporated into a polyurethane (PU) (VUKOL 022) matrix and its subsequent changes in complex permittivity. Two types of surface modification of SiO<sub>2</sub> fillers were investigated. The frequency dependence of the real and imaginary parts of complex permittivity was measured within the frequency range of 1 mHz to 1 MHz using the capacitance method. The 1 wt.% NPs in PU caused an increase (MgO, TiO<sub>2</sub>, n-SiO<sub>2</sub>, and f-SiO<sub>2</sub>) or a decrease (d-SiO<sub>2</sub>) in the real permittivity. The  $\alpha$ -relaxation and intermediate dipolar effect were observed at the temperature dependence of the imaginary permittivity. The change in permittivity by various surface modifications of SiO<sub>2</sub> and other nanofillers was discussed based on the multi-core model. Moreover, the NPs caused a shift in the local maximum of the permittivity, which was a result of the interfacial polarisation and a charge multiplication of the  $\alpha$ -relaxation process.

**INDEX TERMS** Polyurethane, nanoparticles, relaxation methods, nanocomposites.

## I. INTRODUCTION

Each high voltage insulation system is a complex system fulfilling various requirements. In the case of transformers, it can be a solid or a combination of solid and liquid insulating components. There are various materials available for transformer insulation. However, the commonly used materials are cellulose paper and mineral oil systems in the case of cast-resin dry-type transformers (polyurethane [PU], epoxy, and silicone resin). The electrical insulation is an important part of transformers, helping both to withstand the high electric fields and ensure the loss of heat dissipation. In the case of paper-oil transformers also helps the liquid component to dissipate the heat, but at the same time, it creates a potential fire risk. The cast-resin dry-type of transformers is one of the most used types of small transformers, exhibiting good mechanical properties, dielectric strength, and moisture tolerance, as well as decreased fire risk, compared to oil-filled transformers [1]. On the other hand, the low thermal conductivity of the electric insulating system of the dry-type transformers creates

an upper power limit. However, in the case of synthetic cast resin, the operational temperature is significantly higher than in the case of cellulose and mineral oil. The final thermal class of this type of transformer is related to the type of resin used [2].

Insulation systems of modern electrical equipment are exposed to operational and environmental stress during operation [3], [4]. The technical lifetime of the transformer mainly depends on the thermal aging of its electric insulation system. The higher the temperature, the higher the aging rate [5]. From the available statistics [6], [7], it has been shown that due to failure their lifetime is not even 18 years, even though 75 % of all collapses were caused by dielectric insulation issues [8]. Today, polymers are most widely adopted as the main insulating materials in the power engineering industry. In comparison with other types of insulating materials, polymers are maintenance free, with higher stability and a low dissipation factor [9], [10].

Epoxy resins (ERs) and PU substances are of interest to academic and industrial research due to their excellent mechanical, electrical, and thermal properties. They have various applications in industry due to their high adhesive

The associate editor coordinating the review of this manuscript and approving it for publication was Guillaume Parent<sup>1</sup>.

strength and their excellent dielectric and mechanical properties. Due to their excellent dielectric properties, they are widely used as electrical insulation materials, and due to their adhesive properties, they are used as a binder for composites [11]–[15]. Today, polymer-based nanodielectric systems are more frequently investigated for their electrical properties because the introduction of nanofillers has indicated several advantages when compared with the similar properties obtained with pure epoxy systems without any particles or with epoxy systems with micrometre-sized fillers. A lot of studies have shown the effect of different types of nanofillers dispersed in polymer composites, which have exhibited markedly improved mechanical [16], [17], thermal [18], [19], optical, and physico-chemical properties due to the nanometre-sized particles obtained by dispersion, when compared with the pure polymers [20], [21]. In the last two decades, the dielectric properties (relative permittivity -  $\epsilon_{re}$  and dielectric loss -  $\tan \delta$ ) of polymer nano-composites have been evaluated. They values were lower than in pure polymers and microcomposites when insulating oxides were used as fillers [22]–[26]. Many studies have clearly shown that adding some volume of nanoparticles (NPs) to ERs improves several characteristics, such as the dimensional stability, dielectric properties, energy dissipation capabilities, and the high-performance stiffness of polymer composites. The modification of polymers by NPs is one method of acquiring better flexibility and better mechanical or electrical properties. The development of PU-based nanocomposites (NCs) has opened up new possibilities in the field of nanotechnology to obtain new features suitable for industry [12], [13]. The main effect of changes in the dielectric properties of NCs is in the interfacial regions surrounding the NPs [27], [28]. Studies of the complex permittivity of NCs as a function of temperature, electric field intensity, or frequency are fundamental in the characterisation of dielectrics [20], [29].

## II. DIELECTRIC SPECTROSCOPY

Polymers consist of various chains, structures, or other segments, which have various charges; therefore, they create permanent or induced dipoles by an electric field. In the AC electric field, these dipoles are caused by various processes, such as  $\gamma$ -,  $\beta$ - and  $\alpha$ -relaxations; interfacial polarisation (IP) relaxation or the Maxwell–Wagner–Sillars (MWS) effect; the intermediate dipolar effect (IDE); and DC conductivity [21], [30], [31]. The fastest  $\gamma$ -relaxation is readily perturbed at low thermal energy (low temperatures) by small entities of phenyl rings and C-H units [32]. The localized fluctuations and the mobility of the side groups of a polymer, or the rotation of polar groups around C-C bonds, are the main parts of  $\beta$ -relaxation [21], [30], [32], [33].  $\alpha$ -Relaxation is the result of micro-scaled Brownian motion of the whole chain, and for sub-Hertz frequencies DC conductivity can sometimes overshadow this relaxation. With increasing temperature, the IDE is observed with medium relaxation times. This mechanism has been previously observed in  $\text{TiO}_2$  or  $\text{ZnO}$  resin micro-composites [31], [33]–[36]. location is intermediate in

the dielectric spectra, lying between the fast and the slow ( $\alpha$ -relaxation and MWS effect) processes; therefore, it is referred to as the IDE.

The addition of NPs to resins has an impact on the polarisation mechanism, which results in a change in the complex permittivity of the NCs. The interactions between NPs and polymer chains lead to the formation of layers in the interfacial region around the NPs. The space charges accumulated at these layers create large dipoles that are able to follow the changes in the external electric field. These dipoles influence on the IP, which is observed at the low-frequency and high-temperature region [37], [38]. The layers around the NPs also have different properties for both phases and can be described by the multi-core model from Tanaka [27], Tanaka *et al.* [40]. From the model results, two facts should be considered for the reduction in relative permittivity. The first one is the reduction of the mobility of dipoles in the polymer is given layers [21], [30], [39] bounded, and bound layers, which are the closest to the surface of the NPs. The reduction in the outer or loose layer is a secondary effect. With a restriction in polymer chain mobility, the material loses its freedom to relax at the applied stress, which causes a decrease in the electrical polarisation and thus the permittivity. With an increasing filler concentration, the higher relative permittivity has a dominant effect, and higher relative permittivity of the NC compared to that of the pure PU [20], [21], [40] is observed. The dominance of the individual impacts mentioned above results from the types of NPs, their surface modification, and their concentration in the NC.

## III. MATERIALS AND METHODS

The samples of NCs were prepared under laboratory conditions using the method of direct dispersion in compliance with the technological procedures described in other work [41]–[44]. This method guarantees the dispersion of NPs in the polymer matrix, even at very low concentrations. The use of ultrasound provides an efficient, clean, and rapid technological procedure for the synthesis of various PUs. Most of the presented articles [20], [24], [25], [29], [22], [33], [41], [45]–[49] prefer this mechanism with ultrasound for the preparation of NCs from different kinds of NPs in polymers. These processing methods are widely used and preferred because they are not very complicated from a laboratory equipment point of view and allow the available commercially preparation of NCs.

For sample preparation, a two-component PU (the VUKOL 022 and hardener agent Vukit M from VUKI a.s. [50]) potting compound has been used. These two components were mixed in a ratio of 100:37. This type of polyol base is used in industry for filling cavities of all kinds and in the construction of electrical equipment. The final NCs consist of PU with 1 wt.% of NPs: titanium dioxide ( $\text{TiO}_2$ ), magnesium oxide ( $\text{MgO}$ ), and silicon dioxide ( $\text{SiO}_2$ ) NPs with various surface treatments [51]. The basic parameters of used NPs are listed in Table 1.

**TABLE 1. Purity, average size, and surface treatment information for the nanoparticles (NPs) used.**

Name	Purity (%)	Radius (nm)	Surface treatment
MgO	≥99	20	-
TiO <sub>2</sub>	≥96	20	SiO <sub>2</sub> + C <sub>19</sub> H <sub>36</sub> O <sub>2</sub>
n-SiO <sub>2</sub>	≥99	20	-
d-SiO <sub>2</sub>	≥98	20	C <sub>2</sub> H <sub>6</sub> Cl <sub>2</sub> Si
f-SiO <sub>2</sub>	≥98	20	C <sub>10</sub> H <sub>20</sub> O <sub>5</sub> Si

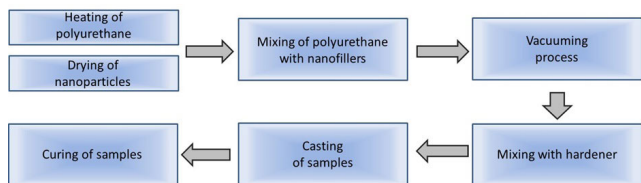


**FIGURE 1. Process of the preparation of polyurethane (PU) nanocomposites (NCs).**

The following describes the fabrication procedure for the test samples. The individual particles were dried in a laboratory hot air oven for 24 h to remove their surface moisture before their incorporation into the polymer. The process of preparing the samples is shown in Fig. 1. The pure PU was then heated to a higher temperature, i.e., 45°C to obtain a lower viscosity, which is better for the direct mixing procedure. After incorporation of the NPs into the PU, the mixture was mixed for 5 h with a magnetic stirrer (700 rpm/min). Furthermore, the vacuuming (8 mbar) process was combined with magnetic stirring and simultaneous heating (50°C, 300 rpm, 4 h). Immediately after completing these processes, the ultrasound needle combined with the vacuuming process for an additional provision of dispersion control was used for 1 h. Then, the hardener agent was added to our mixture in the recommended ratio. In the final step the mixture was poured into the flat form with a dimension 100 × 100 × 1.1 mm was created. From each prepared concentration of the NCs, four pieces of samples were made for repeated measurement and confirmation of the measured results. The final samples were cured under laboratory conditions (23°C, 53% RH) for 48 hours.

The verifications of particle dispersion were performed with the desktop SEM microscope Phenom ProX (ThermoFisher Scientific, Breda, The Netherlands), which was equipped with a backscattered electron detector. Observations were made in charge reduction mode via an optional low vacuum sample holder and with an applied acceleration voltage of 15 kV. The particle distribution in PU is presented for selected samples (Fig. 2) after additional adjustment in graphical software to highlight the MgO, TiO<sub>2</sub>, and SiO<sub>2</sub> NPs where the PU is ideally displayed as a black area. From this image, it is visible that the micrometric agglomerates are present regardless of whether the particles are surface treated. Nevertheless, their distribution within the volume of the material is uniform. This is due to the relatively high viscosity of the polyol base material that was used ( $\eta > 900$  mPa.s [50]).

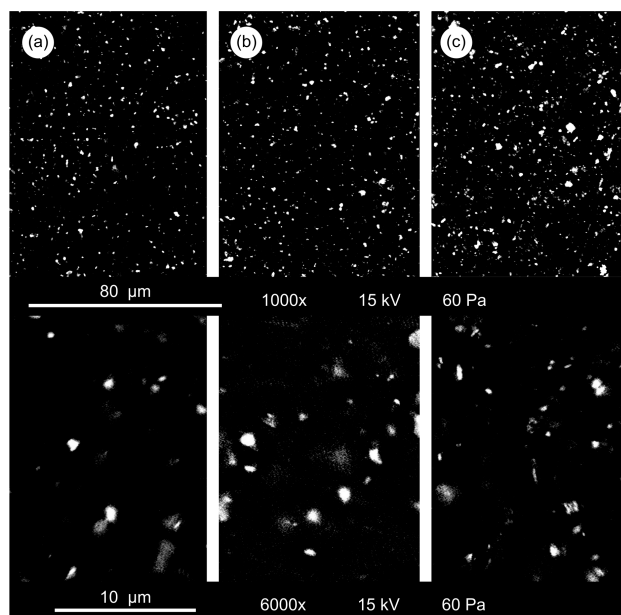


**FIGURE 2. SEM images of nanoparticles distributed in polyurethane: (a) Magnesium oxide, (b) Titanium dioxide treated with SiO<sub>2</sub> + C<sub>19</sub>H<sub>36</sub>O<sub>2</sub>, and (c) Silicon dioxide treated with C<sub>10</sub>H<sub>20</sub>O<sub>5</sub>Si.**

A three-electrode system with a diameter of 38 mm was used for frequency dielectric spectroscopy measurements. Using an LCR Meter OT 7600 Plus at frequencies from 100 Hz to 1 MHz, dielectric parameters such as the real capacitance and resistivity were measured. For the lower frequency range from 1 mHz to 10 kHz, the complex capacitance and dissipation factor were measured by IDAX 350. Tettex 2840 High Precision C and Tan D Measuring Bridge were used for the study of the effect of temperature on the real capacitance and dissipation factor at a frequency 50 Hz.

#### IV. EXPERIMENTAL RESULTS

Since surfaces of NPs are highly active, a significant change in the electrical properties of the NCs can also occur at low nanofiller concentrations. For better characterisation of the influence of NPs on the dielectric properties of the pure PU, we first describe the frequency characteristics of its complex permittivity. The frequency dependence of its relative real and imaginary components for the temperature range of 20-100 °C is depicted in Fig. 3. Within the studied frequency range, the change in complex permittivity was strongly dependent on the frequency and the temperature. The relative real component of the complex permittivity ( $\epsilon_{re}$ ) of pure PU was of 4.3 at 20°C and the frequencies above 10 kHz (Fig. 3a). With a decrease in frequency,  $\epsilon_{re}$  gradual increased, and for frequencies below 10 mHz it was almost frequency-independent with a value of 6.6 (a frequency-independent area). The whole evolution of  $\epsilon_{re}$  shifted to higher frequencies with temperature. This shift is caused by an increase in the rotational and vibrational motion of PU chains with increasing temperature. At temperatures of 60°C and higher, two local maxima were observed, which moved to higher frequencies with temperature, where their

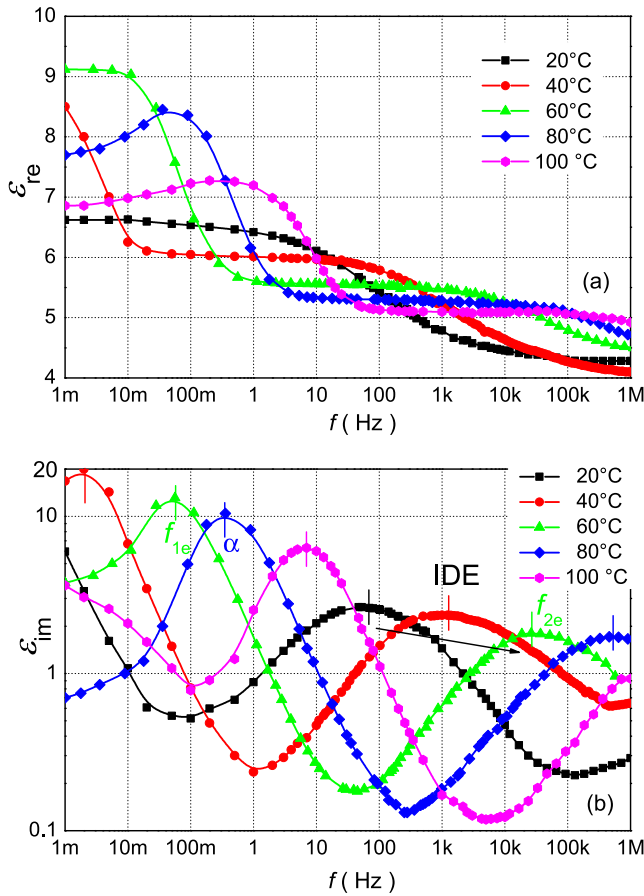


**FIGURE 3.** The frequency dependence of the real (a) and the imaginary (b) part of the complex permittivity for pure PU at various temperatures.

peak values decreased. The increase in  $\epsilon_{re}$  for frequencies below 10 mHz is caused by the influence of DC conductivity or electrode polarization [52].

For better determination of individual polarization processes, Fig. 3b) shows the frequency dependence of the imaginary component of the complex permittivity ( $\epsilon_{im}$ ) on temperature. At 20 °C, we observed two significant effects: a rapid increase in  $\epsilon_{im}$  at sub-Hertz frequencies, which was caused by DC conductivity, together with electrode polarisation and a local maximum around 80 Hz, which is characterised by the eigenfrequency  $f_{2e}$  [ $f_e = 1/(2\pi\tau_0)$ ,  $\tau_0$  is a characteristic time of relaxation process]. Based on the literature [30], [31], [33], [34], we can assign this local maximum to the IDE relaxation process (the internal dipolar effect of polymer chains). With increasing temperature, we observed the local maximum significant shift to higher frequencies (indicated by an arrow) and a slight decrease in its amplitude. At temperatures above 40 °C, another local maximum due to  $\alpha$ -relaxation at the eigenfrequency  $f_{1e}$  was created [33], [34], [47]. With increasing temperature, the mobility of the chains increases, and, thus, there is a decrease in the corresponding relaxation times, which is reflected in the increase in their eigenfrequencies.

The NPs have a significant influence on the dielectric properties of NCs, and from a practical point of view, their

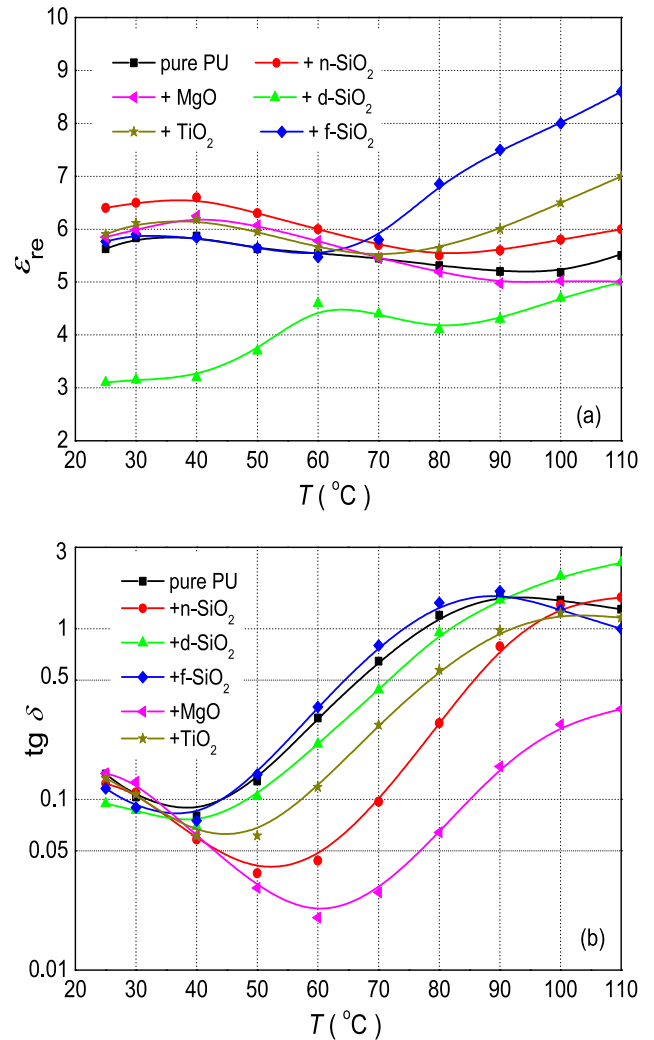


**FIGURE 4.** Temperature dependence of the real part of the complex permittivity (a) and  $\text{tg } \delta$  (b) for PU and its various mixtures with 1 wt.% NPs measured at a frequency of 50 Hz.

effects on  $\epsilon_{re}$  and  $\text{tg } \delta$  at only a single frequency (50 Hz) depending on temperature were first studied (Fig. 4). In this type of measurement, the temperature was varied from 25-110°C. The  $\epsilon_{re}$  of the pure PU at the studied temperature range was almost constant (Fig. 4a). From this measurement is evident that d-SiO<sub>2</sub> filler caused significant decrease of  $\epsilon_{re}$ . The lower value of  $\epsilon_{re}$  also guarantees a lower level of local stress inside the electrical insulation system. Other fillers had the same or higher value of  $\epsilon_{re}$  for temperatures below 70°C. The  $\epsilon_{re}$  increased due to  $\alpha$ -relaxation at higher temperatures in all NCs.  $\text{tg } \delta$  of pure PU decreases at temperatures 25 - 40°C. At 40 °C, it reached a local minimum and then it increases with temperature (Fig. 4b). This local minimum moves to higher temperatures only for n-SiO<sub>2</sub> and MgO fillers. At temperatures above 70°C, a gradual increase in  $\text{tan } \delta$  can be seen in all NCs.

Fig. 5 shows the frequency dependence of the complex permittivity of PU with 1 wt.% of the n-SiO<sub>2</sub> filler as a function of temperature. The extreme increase in  $\epsilon_{re}$  at low



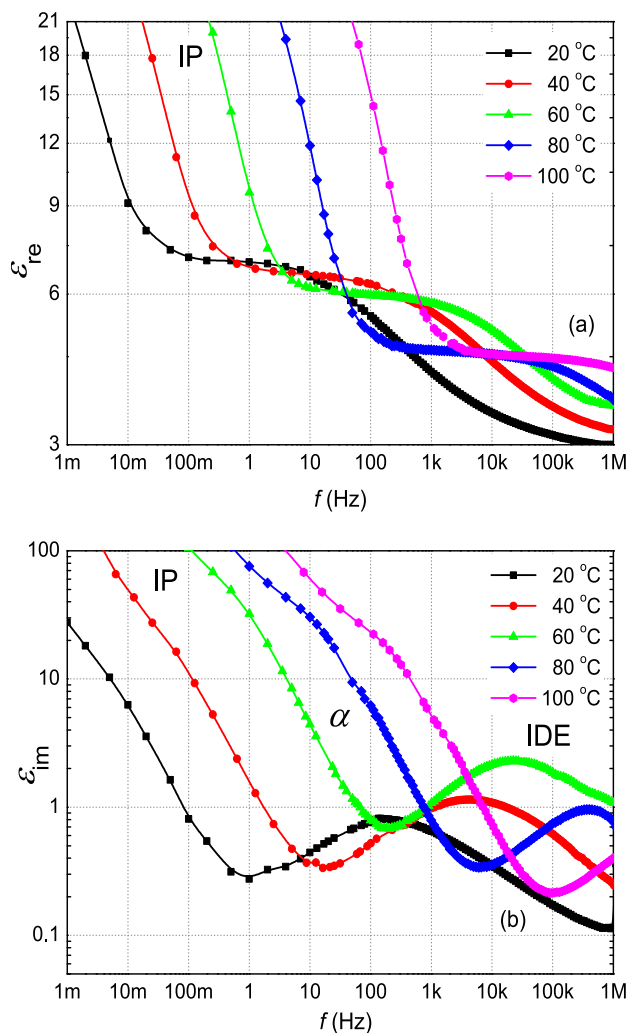


**FIGURE 5.** The frequency dependence of the real (a) and the imaginary (b) part of the complex permittivity for PU with 1 wt.% n-SiO<sub>2</sub> nanoparticles.

frequencies is the main effect, which can be seen in Fig. 5a). In the case of pure PU (Fig. 3a), at all frequencies  $\epsilon_{re}$  was less than 10. This increase is caused by IP around NPs, and with temperature it moves to higher frequencies. This effect was also observed in other works [22], [33], [53]. The frequency-independent area of  $\epsilon_{re}$  at 20°C was in the frequency range of 100 mHz to 10 Hz, then gradually decreased with frequency and from 100 kHz  $\epsilon_{re}$  had a value 3. As temperature increased, the frequency-independent area shifted to higher frequencies and its values decreased. At 20°C,  $\epsilon_{im}$  had a local maximum at a frequency of around 300 Hz (IDE relaxation process), and it increased with temperature to higher frequencies Fig. 5b). The effect of the  $\alpha$ -relaxation process is highlighted by IP and  $\epsilon_{im}$  extremely increased for low frequencies. For other surface modifications and fillers, similar characteristics have been observed [54], [55] and the comparisons are shown in Figs. 6, 7.

Fig. 6 shows the frequency dependence of the complex permittivity of pure PU and with 1 wt.% of SiO<sub>2</sub> of various surface modification (Table 1), and their dielectric parameters

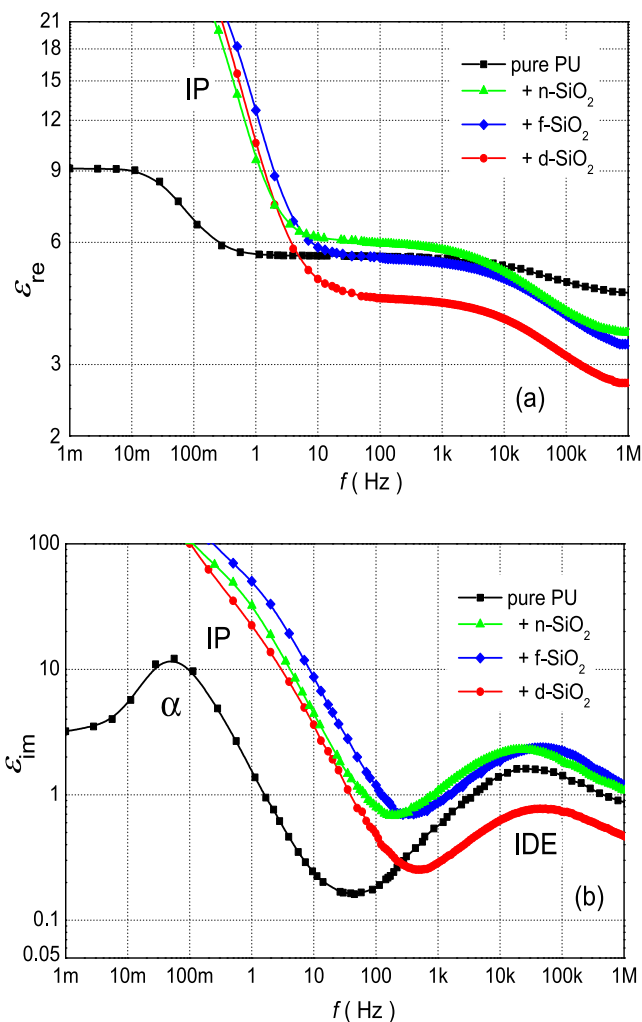


**FIGURE 6.** The frequency dependence of the real (a) and the imaginary (b) part of the complex permittivity for PU and its mixture of 1 wt.% of SiO<sub>2</sub> NPs with various surface modifications at the temperature 60°C.

obtained from the Cole-Cole model (Eq. 1) are listed in Table 2. The  $\epsilon_{re}$  of the mixture of PU and n-SiO<sub>2</sub> (without surface modification) was almost the same as for pure PU in the frequency range from 10 Hz to 10 kHz and then decreased. In the case of d-SiO<sub>2</sub> (surface modification with dimethyldichlorosilane), there is a marked decrease of  $\epsilon_{re}$  for frequencies above 4 Hz. The  $\epsilon_{re}$  of the NC with f-SiO<sub>2</sub> (second surface modification with 3-(Trimethoxysilyl)propyl methacrylate) was similar to that of n-SiO<sub>2</sub>. For lower frequencies, higher values were observed due to IP, as for other NPs (Fig. 7). The development of  $\epsilon_{im}$  for pure PU has two local maxima (Fig. 3b). As can be seen from Fig. 6b), the SiO<sub>2</sub> filler and its surface modification had some effect on the position of the second maximum (Table 2). In the case of d-SiO<sub>2</sub>, an important decrease according to pure PU was observed. For the first maximum, the situation was different: there was a significant shift to higher frequencies (Table 2).

However, real dielectrics have several variations of dipole molecules in different configurations; their relaxation times

**TABLE 2.** Parameters obtained from the fit by the Cole-Cole model for pure PU and its various types of NPs at 60°C [ $\epsilon_\infty$  is the high-frequency limit of the permittivity,  $\sigma_{DC}$  is the DC conductivity ( $10^{-12}$  S/m),  $\tau$  is the relaxation time, and  $\alpha$  is the shape parameter].

Parameter	unit	pure PU	+n-SiO <sub>2</sub>	+d-SiO <sub>2</sub>	+f-SiO <sub>2</sub>	+MgO	+TiO <sub>2</sub>
$\epsilon_\infty$		4.3	3.6	2.7	3.2	3.0	4.0
$\sigma_{DC}$	$10^{-12}$ S/m	0.27	372	283	510	2.39	88.6
$\tau_1$	s	2.87	0.80	0.94	1.12	23.4	1.84
$f_{1e}$	mHz	60	200	210	220	9	100
$a_1$		0	0.02	0.23	0.05	0.05	0.6
$\tau_2$	$\mu$ s	5.9	6.7	3.0	3.3	6.1	2.5
$f_{2e}$	kHz	276	23	54	48	26	64
$a_2$		0.05	0.35	0.2	0.38	0.4	0.4

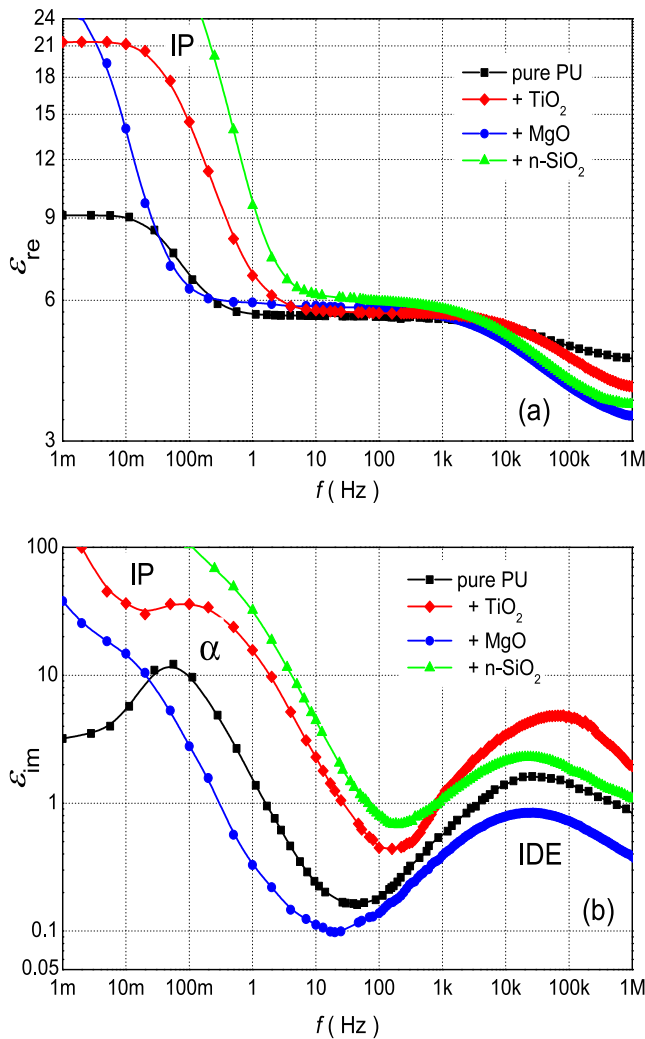


**FIGURE 7.** The frequency dependence of the real (a) and the imaginary (b) part of the complex permittivity for PU and its mixtures of 1 wt.% with various NPs at 60°C.

have some distribution. Parameters that characterise PU and NCs can be obtained from the fits of the complex permittivity. We used the Cole-Cole model, which has been widely used by other authors [32], [33], [47]. The resulting relation for the complex permittivity according to the Cole-Cole distribution with two relaxation process has the following form:

$$\epsilon^* = \epsilon_\infty - j \frac{\sigma_{DC}}{\epsilon_0 \omega} + \frac{\Delta \epsilon_1}{1 + (j\omega\tau_1)^{1-a_1}} + \frac{\Delta \epsilon_2}{1 + (j\omega\tau_2)^{1-a_2}} \quad (1)$$

where  $\epsilon_\infty$  is the high-frequency limit of the permittivity,  $\sigma_{DC}$  is the DC conductivity,  $\omega$  represents the angular frequency,  $\epsilon_0$  is the permittivity of a vacuum,  $\Delta \epsilon$  is the difference of the low- and high-frequency limit of the permittivity,  $\tau$  is the relaxation time,  $a$  represents the dispersion index of the relaxation time, and the subscripts 1 and 2 represent the  $\alpha$ -relaxation and IDE relaxation processes, respectively. The calculated parameters for the studied NCs are listed in Table 2. The bond and loose layers of the NPs caused an extension of the second peak, which corresponds to an increase in  $a_2$ .

The next type of measurement was focused on the influence of various NPs on the complex permittivity of pure PU. Its frequency dependence 60°C is shown in Fig. 7, and the parameters obtained from the Cole-Cole model (Eq. 1) are in Table 2. Within the frequency range, the changes in the complex permittivity depend on the type of NP. In the frequency range from 8 Hz to 1 kHz,  $\epsilon_{re}$  of all NCs was almost the same as pure PU. The  $\epsilon_{re}$  of the NCs for sub-Hertz frequencies increased. This increase was caused by IP in the layers around the NPs, where the bound charges increased a local electric field and  $\alpha$ -relaxation process was enhanced. This effect was named as a charge multiplication of  $\alpha$ -relaxation process. NCs with TiO<sub>2</sub> and n-SiO<sub>2</sub> fillers had higher values of  $\epsilon_{im}$  across the whole frequency range. Their next effect is a slight shift in the first local maximum of  $\epsilon_{im}$  to higher frequencies (Table 2). In the case of MgO, the conductivity was one order of magnitude lower than in other NCs. This caused a shift of the first low-frequency maximum to lower frequencies and a significant decrease in  $\epsilon_{im}$  to pure PU, except for the sub-Hertz frequencies. The position and the value of the second local maximum corresponding to the IDE relaxation process were also influenced by the type of NPs.

## V. DISCUSSION

Our measurements show several results. Firstly, the addition of NPs in a commercially used resin, PU VUKOL 022, caused a significant increase in the relative permittivity for frequencies below 10 Hz. Secondly, the relative permittivity of the NC (PU + 1 wt.% d-SiO<sub>2</sub>) was lower than pure PU at all temperatures at the basic operating frequency of 50 Hz (Fig. 3a) and for frequencies of over 10 Hz at the temperature of 60°C (Fig. 6a). The second surface modification of f-SiO<sub>2</sub> and other NPs in the frequency range from 50 Hz to 1 kHz have a

similar  $\varepsilon_{re}$  or slightly higher than pure PU (Figs. 6a, 7a)).  $\text{SiO}_2$  and its surface modifications caused a more pronounced shift of the eigenfrequency of the  $\alpha$ -relaxation process to higher frequencies (Fig. 6b), while at the MgO filler it was shifted to a lower frequency (Table 2, Fig. 7b). Based on  $\alpha$ -relaxation and IDE relaxation processes and experimental and theoretical studies of other authors, the influence of NPs and their surface treatments on the studied dielectric parameters are described in the following sections.

From a practical point of view in the next step, we focused on the change of  $\varepsilon_{re}$  and  $\text{tg } \delta$  with temperature in the studied NCs for the frequency of 50 Hz (Fig. 4). Up to  $70^\circ\text{C}$ , the  $\varepsilon_{re}$  of the NCs was slightly higher compared to pure PU; it was smaller only for the d- $\text{SiO}_2$  filler. This observed difference can be explained by the multi-core model described by Tanaka [27], Tanaka *et al.* [56]. Surface modification of  $\text{SiO}_2$  by dimethyldichlorosilane caused a better connection with PU chains; therefore, they were more strongly bound in the bounded layer around the NP than for n- $\text{SiO}_2$  (without surface modification). The presence of these highly immobile PU chains in the interfacial (bounded and bound layers) regions [21] caused the observed decrease of  $\varepsilon_{re}$ . This effect was observed in NCs with a concentration of filler below 1 wt.% [54] when a bounded movement of chains was more pronounced than the NP permittivity. For the other types of studied NPs, the bound effect of chains was not so significant. In these cases the influence of permittivity of NPs was more noticeable and NCs had a similar permittivity as pure PU. The increase in  $\varepsilon_{re}$  for pure PU and the NCs from  $70^\circ\text{C}$  was caused by the  $\alpha$ -relaxation process; for temperatures higher than  $90^\circ\text{C}$ , this was caused by  $\gamma$ -conductivity [21]. The position of the local minimum of  $\text{tg } \delta$  was dependent on the type of filler in the NC, and it was at higher temperature for MgO fillers. This effect was connected with the shift of the  $\alpha$ -relaxation process to lower frequencies (Figs. 6, 7) [49].

Fig. 6 shown the effect of surface treatment of  $\text{SiO}_2$  NPs (Table 1) on the complex permittivity of the NCs. From Fig. 4, it is evident that each surface treatment had a different effect on permittivity value. Firstly, we can see that  $\varepsilon_{re}$  of the NC with n- $\text{SiO}_2$  at 50 Hz was higher than that of pure PU for the studied temperatures. This increase is the result of the higher relative permittivity of the n- $\text{SiO}_2$  filler than that of pure PU. In the studied frequency range at  $60^\circ\text{C}$  (Fig. 6), the situation was different for frequencies below 10 Hz. A large increase is the influence of the charge multiplication of  $\alpha$ -relaxation processes due to IP at the surface of the NPs [57]. Due to the binding of PU chains on the NPs, they appear to have a larger radius. This effect increased the impact of IP around each NP, and a visible increase in  $\varepsilon_{re}$  at frequencies below 5 Hz was measured. The larger radius and surface modification accelerated the  $\alpha$ -relaxation process, and a decrease of relaxation time ( $\tau_1$ ) and a shift of  $\varepsilon_{im}$  to higher frequencies (Fig. 6b, Table 2) were observed. The IDE relaxation process or the positions of the second local maximum were slightly affected, but in the case of d- $\text{SiO}_2$   $\varepsilon_{im}$  dropped significantly for frequencies over 500 Hz (Fig. 6b).

The d- $\text{SiO}_2$  had the most striking effect on the decrease of  $\varepsilon_{re}$  for frequencies above 4 Hz. This decrease meant that this surface modification was very effective for the bonding of PU chains to the surface of NPs and changes in the degree of crosslinking due to the reaction of polymeric groups. They react with the coupling agent molecules on the NP surface and form a linear polymer chain in the interphase region [21], [49]. A higher bonding effect is connected with a decrease in the mobility of PU chains in the interfacial region (bounded and bound layers) around the NPs. The f- $\text{SiO}_2$  filler caused a slight decrease in  $\varepsilon_{re}$  in consideration of n- $\text{SiO}_2$  for frequencies over 10 Hz; therefore, this surface modification had a similar influence on the bonding effect of PU chains as n- $\text{SiO}_2$ .

The last measurement was focused on the influence of various types of NPs (Table 1) on the complex permittivity of PU at  $60^\circ\text{C}$  (Fig. 7). At sub-Hertz frequencies, there was a significant increase in  $\varepsilon_{re}$  for all types of NPs by the charge multiplication of  $\alpha$ -relaxation process due to IP at the NPs surface. The influence of NPs is also visible in the development of  $\varepsilon_{im}$ . There was a decrease for the MgO filler and an increase for n- $\text{SiO}_2$  and  $\text{TiO}_2$  fillers. The shift of the position of the  $\alpha$ -relaxation process ( $\tau_1$  in Table 2) depended on the type of NPs. NCs are materials prone to IP; therefore, space-charge build-up occurs at the macroscopic interfaces as a result of the difference in conductivities and permittivities of the constituents. These trapped charges (electrons and ions) [49] at the interface of the NP and PU matrix (bound and released layers) create a local electric field around the NP (the charge multiplication). This field is higher than Laplacian or geometric electric fields; therefore, it influences the reorientation of the electric dipoles of PU chains bound in layers around the NP. The higher electric field causes a faster transfer of dipole charges, which is reflected by the shift of the local maximum caused by the  $\alpha$ -relaxation process to higher frequencies, and  $\varepsilon_{re}$  increases more markedly at low frequencies. The decrease in the case of MgO is caused by an increase in the energy levels of the electron traps [57], which results in a higher resistance (low  $\sigma_{DC}$ ) to charge accumulation in the inner structure of the material. The position of the second local maximum, the IDE-relaxation process, was also influenced by the fillers (Fig. 6b). For MgO, its value was lower than for pure PU, while  $\text{TiO}_2$  was around three times higher due to its high permittivity.

## VI. CONCLUSION

Dielectric spectroscopy for the study of PU NCs with various surface modifications of  $\text{SiO}_2$  and types of NPs as fillers was used. This can help to understand basic issues related to the role of additives, their surface modification, and interactions with a two-component PU matrix. The values of the complex permittivity of the NCs measured within the frequency range of 1 mHz to 1 MHz and temperature were dependent on the types of NPs and the surface modification. For a description of the observed changes in the dielectric properties of PU NCs, the multi-core model of the NCs and the influence of

a local electric field on the trapped charges were used. In the case of the d-SiO<sub>2</sub> filler, the complex permittivity was lower than for other fillers. The decrease in the relative permittivity was caused by the presence of highly immobile PU chains in the interfacial regions around the NPs. The effects of the  $\alpha$ -relaxation and IDE relaxation processes were identified with dielectric spectroscopy. The IP and charge multiplication of  $\alpha$ -relaxation process for all types of NPs caused the shifts of the peak and a marked increase in the relative permittivity,  $\epsilon_{re}$ , for sub-Hertz frequencies.

## REFERENCES

- [1] R. Mafra, E. Magalhães, B. Anselmo, F. Belchior, and S. L. Silva, "Winding hottest-spot temperature analysis in dry-type transformer using numerical simulation," *Energies*, vol. 12, no. 1, p. 68, Dec. 2018.
- [2] S. K. Kumar, B. C. Benicewicz, R. A. Vaia, and K. I. Winey, "50th anniversary perspective: Are polymer nanocomposites practical for applications?" *Macromolecules*, vol. 50, no. 3, pp. 714–731, Feb. 2017.
- [3] L. Harvanek, V. Mentlik, P. Trnka, and J. Hornak, "Effect of electrical/thermal aging on dielectric properties of polymer/SiO<sub>2</sub> nanocomposites," in *Proc. IEEE Int. Conf. Dielectr. (ICD)*, vol. 2, Jul. 2016, pp. 92–95.
- [4] V. Mentlik, P. Trnka, M. Svoboda, J. Hornak, P. Totzauer, and L. Harvanek, "Aging phenomena of paper-oil insulating system under different voltage stress," in *Proc. IEEE 11th Int. Conf. Properties Appl. Dielectr. Mater. (ICPADM)*, Sydney, NSW, Australia, Jul. 2015, pp. 548–551.
- [5] X. Ding and W. Ning, "Analysis of the dry-type transformer temperature field based on fluid-solid coupling," in *Proc. 2nd Int. Conf. Instrum., Meas., Comput., Commun. Control*, Dec. 2012, pp. 520–523.
- [6] M. Rafiq, Y. Lv, and C. Li, "A review on properties, opportunities, and challenges of transformer oil-based nanofluids," *J. Nanomater.*, vol. 2016, pp. 1–23, Jul. 2016.
- [7] W. H. Bartley, "Investigating transformer failure," in *Proc. Weidmann-ACI 5th Annu. Tech. Conf. New Diagnostic Concepts Better Asset Manage.*, Albuquerque, NM, USA, Nov. 2006.
- [8] *EPRI Portfolio 2007 Transmission Reliability and Performance: 37.002, Transformer Life Extension*. Accessed: Dec. 12, 2020. [Online]. Available: <http://www.epri.com/portfolio/>
- [9] A. Küchler, "Insulating materials," in *High Voltage Engineering: Fundamentals-Technology-Applications*, New York, NY, USA: Springer-Verlag GmbH, 2018, 10.1007/978-3-642-11993-4.
- [10] R. S. A. Afia, E. Mustafa, and Z. A. Tamus, "Mechanical stresses on polymer insulating materials," in *Proc. Int. Conf. Diag. Electr. Eng. (Diagnostika)*, Pilsen, Czech Republic: IEEE Press, Sep. 2018, pp. 1–4.
- [11] J. Mleziva, *Polymery a Vyroba, Struktura, Vlastnosti a Pouziti*. Praha, Slovakia: Sobotales, 1993.
- [12] O. Becker and G. P. Simon, "Epoxy nanocomposites based on layered silicates and other nanostructured fillers," in *Polymer Nanocomposites*, Feb. 2006, ch. 2, pp. 29–35, doi: 10.1533/9781845691127.1.29.
- [13] R. Ramprasad, N. Shi, and C. Tang, "Modeling the physics and chemistry of interfaces in nanodielectrics," in *Dielectric Polymer Nanocomposites*, J. K. Nelson, Ed. San Jose, CA, USA: Springer-Verlag, 2010, pp. 133–161.
- [14] P. Bartko, M. Rajnák, R. Cimbala, K. Paulovicová, M. Timko, P. Kopcanský, and J. Kurimský, "Effect of electrical polarity on dielectric breakdown in a soft magnetic fluid," *J. Magn. Magn. Mater.*, vol. 497, Mar. 2020, Art. no. 166007.
- [15] A. Baran, P. Vrábel, M. Kovalaková, M. Hutníková, O. Fricová, and D. Olcák, "Effects of sorbitol and formamide plasticizers on molecular motion in corn starch studied using NMR and DMTA," *J. Appl. Polym. Sci.*, vol. 137, no. 33, p. 48964, Sep. 2020.
- [16] T. K. Saha and P. Purkait, "Transformer insulation materials and ageing," in *Transformer Ageing: Monitoring and Estimation Techniques* T. K. Saha and P. Purkait, Eds. Singapore: Wiley, 2017, pp. 1–35.
- [17] M. Kim, S. Kim, T. Kim, D. Lee, B. Seo, and C.-S. Lim, "Mechanical and thermal properties of epoxy composites containing zirconium oxide impregnated halloysite nanotubes," *Coatings*, vol. 7, no. 12, p. 231, Dec. 2017.
- [18] N. Domun, K. Paton, H. Hadavinia, T. Sainsbury, T. Zhang, and H. Mohamud, "Enhancement of fracture toughness of epoxy nanocomposites by combining nanotubes and nanosheets as fillers," *Materials*, vol. 10, no. 10, p. 1179, Oct. 2017.
- [19] X. Zhang, H. Wen, and Y. Wu, "Computational thermomechanical properties of silica-epoxy nanocomposites by molecular dynamic simulation," *Polymers*, vol. 9, no. 12, p. 430, Sep. 2017.
- [20] S. Singha and M. Thomas, "Dielectric properties of epoxy nanocomposites," *IEEE Trans. Dielectr. Electr. Insul.*, vol. 15, no. 1, pp. 12–23, Feb. 2008.
- [21] R. Kochetov, "Thermal and electrical properties of nanocomposites, including material processing," Ph.D. dissertation, Electr. Eng., Math. Comput. Sci., Saint-Petersburg State Electrotech. Univ., Saint Petersburg, Russia, 2012.
- [22] X. Wang, Q. Chen, H. Yang, K. Zhou, and X. Ning, "Electrical properties of epoxy/ZnO nano-composite," *J. Mater. Sci., Mater. Electron.*, vol. 29, no. 15, pp. 12765–12770, Aug. 2018.
- [23] A. K. Fedotov, A. V. Pashkevich, J. A. Fedotova, A. S. Fedotov, T. N. Koltunowicz, P. Zukowski, A. A. Ronassi, V. V. Fedotova, I. A. Svito, and M. Budzynski, "Electron transport and thermoelectric properties of ZnO ceramics doped with Fe," *J. Alloys Compounds*, vol. 854, Feb. 2021, Art. no. 156169.
- [24] J.-J. Park, "Electrical properties of epoxy composites with micro-sized fillers," *Trans. Electr. Electron. Mater.*, vol. 19, no. 6, pp. 475–480, Dec. 2018.
- [25] Y. R. Eker, M. Özcan, A. Ozcan, and H. Kirkici, "The influence of Al<sub>2</sub>O<sub>3</sub> and TiO<sub>2</sub> additives on the electrical resistivity of epoxy resin-based composites at low temperature," *Macromol. Mater. Eng.*, vol. 304, Jul. 2019, Art. no. 1800670.
- [26] M. Awais, R. Sundararajan, I. A. Sajjad, S. S. Haroon, S. Amin, H. Shaikat, and M. A. Nasir, "Investigation on optimal filler loadings for dielectric strength enhancement of epoxy/TiO<sub>2</sub>@SiO<sub>2</sub> nanocomposite," *Mater. Res. Exp.*, vol. 6, no. 6, Mar. 2019, Art. no. 065709.
- [27] T. Tanaka, "Dielectric nanocomposites with insulating properties," *IEEE Trans. Dielectr. Electr. Insul.*, vol. 12, no. 5, pp. 914–928, Oct. 2005.
- [28] J. K. Nelson, J. C. Fothergill, L. A. Dissado, and W. Peasgood, "Towards an understanding of nanometric dielectrics," in *Proc. Annu. Rep. Conf. Electr. Insul. Dielectr. Phenomena*, Cancun, Mexico, Oct. 2002, pp. 295–298.
- [29] S. Mallakpour and V. Behranvand, "Polymeric nanoparticles: Recent development in synthesis and application," *Exp. Polym. Lett.*, vol. 10, no. 11, pp. 895–913, 2016.
- [30] A. K. Jonscher, "Dielectric relaxation in solids," *J. Phys. D, Appl. Phys.*, vol. 32, no. 14, pp. R57–R70, 1999.
- [31] G. N. Tomara, A. P. Kerasidou, A. C. Patsidis, P. K. Karahaliou, G. C. Psarras, S. N. Georga, and C. A. Krontiras, "Dielectric response and energy storage efficiency of low content TiO<sub>2</sub>-polymer matrix nanocomposites," *Compos. A, Appl. Sci. Manuf.*, vol. 71, pp. 204–211, Apr. 2015.
- [32] Y. Ahmad, "Polymer dielectric materials," in *Dielectric Material*, M. A. Silaghi, Ed. London, U.K.: IntechOpen, 2011, doi: 10.5772/50638.
- [33] A. Soulintzis, G. Kontos, P. Karahaliou, G. C. Psarras, S. N. Georga, and C. A. Krontiras, "Dielectric relaxation processes in epoxy resin-ZnO composites," *J. Polym. Sci. B, Polym. Phys.*, vol. 47, no. 4, pp. 445–454, Feb. 2009.
- [34] G. A. Kontos, A. L. Soulintzis, P. K. Karahaliou, G. C. Psarras, S. N. Georga, C. A. Krontiras, and M. N. Pisanias, "Electrical relaxation dynamics in TiO<sub>2</sub>-polymer matrix composites," *Exp. Polym. Lett.*, vol. 1, no. 12, pp. 781–789, 2007.
- [35] L. A. Ramajo, A. A. Cristóbal, P. M. Botta, J. M. P. López, M. M. Reboredo, and M. S. Castro, "Dielectric and magnetic response of Fe<sub>3</sub>O<sub>4</sub>/epoxy composites," *Compos. A Appl. Sci. Manuf.*, vol. 40, no. 4, pp. 388–393, 2009.
- [36] M. Hernández, T. A. Ezquerro, R. Verdejo, and M. A. López-Manchado, "Role of vulcanizing additives on the segmental dynamics of natural rubber," *Macromolecules*, vol. 45, no. 2, pp. 1070–1075, Jan. 2012.
- [37] K. W. Wagne, "Erklärung der dielektrischen nachwirkungsvorgänge auf grund maxwellscher vorstellungen," *Arch. Elektrotech.*, vol. 2, no. 9, pp. 371–387, 1914.
- [38] R. W. Sillars, "The properties of a dielectric containing semiconducting particles of various shapes," *J. Inst. Electr. Eng.*, vol. 80, no. 484, pp. 378–394, Apr. 1937.



- [39] P. Pissis, "Molecular dynamics of thermoset nanocomposites," in *Thermoset Nanocomposites for Engineering Application*. London, U.K.: Smithers Rapra Technology, 2007, pp. 143–206.
- [40] T. Tanaka, G. C. Montanari, and R. Malhaupt, "Process, understanding and challenges in the field of nanodielectrics," *IEEE Trans. Dielectr. Electr. Insul.*, vol. 11, no. 5, pp. 763–784, 2004.
- [41] M. M. Rahman, "Polyurethane/Zinc oxide (PU/ZnO) composite—Synthesis, protective property and application," *Polymers*, vol. 12, no. 7, p. 1535, Jul. 2020.
- [42] S. A. Mogy, R. S. Youssef, and A. Megeed, "Processing of polyurethane nanocomposite reinforced with nanosized zinc oxide: Effect on mechanical and acoustic properties," *Egypt. J. Chem.*, vol. 62, no. 2, pp. 333–341, 2019.
- [43] Y. Zhou, X. Wang, X. Liu, D. Sheng, F. Ji, L. Dong, S. Xu, H. Wu, and Y. Yang, "Multifunctional ZnO/polyurethane-based solid-solid phase change materials with graphene aerogel," *Sol. Energy Mater. Sol. Cells*, vol. 193, pp. 13–21, May 2019.
- [44] S. Zhang, D. Zhang, H. Bai, and W. Ming, "ZnO nanoparticles coated with amphiphilic polyurethane for transparent polyurethane nanocomposites with enhanced mechanical and UV-shielding performance," *ACS Appl. Nano Mater.*, vol. 3, no. 1, pp. 59–67, Jan. 2020.
- [45] S. Strachan, S. Rudd, S. McArthur, M. Judd, S. Meijer, and E. Gulski, "Knowledge-based diagnosis of partial discharges in power transformers," *IEEE Trans. Dielectr. Electr. Insul.*, vol. 15, no. 1, pp. 259–268, Feb. 2008.
- [46] H. Shi, N. Gao, H. Jin, G. Zhang, and Z. Peng, "Investigation of the effects of nano-filler on dielectric properties of epoxy based composites," in *Proc. IEEE 9th Int. Conf. Properties Appl. Dielectr. Mater.*, Jul. 2009, pp. 804–807.
- [47] M. Klampár and K. Liedermann, "Dielectric relaxation spectroscopy of epoxy resins with TiO<sub>2</sub>, Al<sub>2</sub>O<sub>3</sub>, WO<sub>3</sub> and SiO<sub>2</sub> nanofillers," in *Proc. IEEE Int. Symp. Electr. Insul.*, San Juan, PR, USA, Jun. 2012, pp. 637–640.
- [48] D. Saha, R. Kochetov, and P. H. F. Morshuis, "Space charge analysis of epoxy-boron nano-composites and the importance of dispersion techniques," in *Proc. IEEE Electr. Insul. Conf. (EIC)*, Jun. 2019, pp. 312–316.
- [49] J. Hornak, P. Trnka, P. Kadlec, O. Michal, V. Mentlík, P. Šutta, G. Csányi, and Z. Tamas, "Magnesium oxide nanoparticles: Dielectric properties, surface functionalization and improvement of epoxy-based composites insulating properties," *Nanomaterials*, vol. 8, no. 6, p. 381, May 2018.
- [50] VUKI. Accessed: Dec. 12, 2020. [Online]. Available: [https://www.vuki.sk/files/technicke\\_listy/TDS-VUKOL-O22-ver-2018-04-30-sk.pdf](https://www.vuki.sk/files/technicke_listy/TDS-VUKOL-O22-ver-2018-04-30-sk.pdf)
- [51] *Nanostructured & Amorphous Materials, Inc.* Accessed: Dec. 12, 2020. [Online]. Available: <https://www.nanoamor.com/>
- [52] R. Raihan, F. Rabbi, V. Vadlamudi, and K. Reifsnider, "Composite materials damage modeling based on dielectric properties," *Mater. Sci. Appl.*, vol. 6, no. 11, pp. 1033–1053, 2015.
- [53] J. Kúdelčík, E. Jahoda, J. Hornak, O. Michal, and P. Trnka, "Partial discharges and dielectric parameters of epoxy resin filled with nanoparticles," in *Proc. 19th Int. Sci. Conf. Electr. Power Eng. (EPE)*, Brno, Czech Republic, May 2018, pp. 1–6.
- [54] J. Kúdelčík, E. Jahoda, and J. Kurimský, "The effect of SiO<sub>2</sub> nano-filler on dielectric properties of epoxy resin," *Eur. Phys. J. Appl. Phys.*, vol. 85, no. 1, p. 10401, Jan. 2019.
- [55] E. Jahoda, J. K. Kúdelčík, J. Hornak, and P. Trnka, "The influence of nanoparticles in the epoxy resin on dielectric parameters and partial discharges," in *Proc. ELEKTRO*, Mikulov, Czech Republic, 2018, pp. 1–5.
- [56] T. Tanaka, A. Bulinski, J. Castellon, M. Frechette, S. Gubanski, J. Kindersberger, G. C. Montanari, M. Nagao, P. Morshuis, Y. Tanaka, and S. Pelissou, "Dielectric properties of XLPE/SiO<sub>2</sub> nanocomposites based on CIGRE WG D1.24 cooperative test result," *IEEE Trans. Dielectr. Electr. Insul.*, vol. 18, no. 5, pp. 1484–1517, Oct. 2011.
- [57] G. Chen, S. Li, and L. Zhong, "Space charge in nanodielectrics and its impact on electrical performance," in *Proc. IEEE 11th Int. Conf. Properties Appl. Dielectr. Mater. (ICPADM)*, Sydney, NSW, Australia, Jul. 2015, pp. 19–22.
- [58] H. Li, C. Wang, Z. Guo, H. Wang, Y. Zhang, R. Hong, and Z. Peng, "Effects of silane coupling agents on the electrical properties of silica/epoxy nanocomposites," in *Proc. IEEE Int. Conf. Dielectr. (ICD)*, Montpelier, France, Jul. 2016, pp. 3–7.



**JOZEF KÚDELČÍK** was born in Ružomberok, Slovakia, in January 1975. He graduated (Mgr.) from the Department of Plasma Physics, Faculty of Mathematics and Physics, Comenius University, Bratislava, in 1998. He received the Ph.D. degree in the field of stage of breakdown in the mixtures with SF<sub>6</sub> in 2003, and the Habilitation degree in electro-technology and materials in 2011. Since 1998, he has been working as a Researcher with the Department of Physics, University of Žilina.

His scientific research interests include discharge mechanism and partial discharge in gases and dielectric, such as water or oil. His second great area of research is the processes in magnetic fluids, liquid crystals, and nanocomposites in a magnetic field studied by acoustic and dielectric spectroscopy.



**ŠTEFAN HARDOŇ** was born in 1988. He graduated from the Department of Telecommunication, University of Žilina. He received the Ph.D. degree in electrotechnologies and materials in 2015, with a focus on exploitation of acoustic techniques at research materials and structures. Since 2015, he has been working as a Researcher with the Department of Physics, University of Žilina. His current research interests include the processes in magnetic fluids in a magnetic field studied by

acoustic and dielectric spectroscopy, and studies of nanocomposites by dielectric spectroscopy.



**PETER HOCKICKO** was born in Levoča, Slovakia, in February 1973. He received the M.Sc. degree (distinction) from the Faculty of Mathematics, Physics and Informatics, Comenius University, Bratislava, in 1996. He defended his Ph.D. theses in the field of physics of condensed matter and acoustics in 2008 and the thesis title was "Study of relaxation processes in matter using acoustic methods." From 1999 to 2012, he worked as a Tutor, a Lecturer, and a Researcher with the

Department of Physics, Faculty of Electrical Engineering and Information Technology, University of Žilina, where he has been working as an Associate Professor, since 2013. His scientific research interest includes relaxation processes in materials.

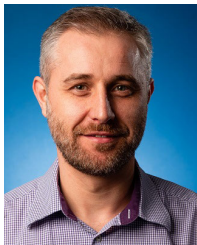


**MÁRIA KÚDELČÍKOVÁ** was born in Žilina, Slovakia, in February 1977. In 2000, she graduated (Ing.) in applied mathematics from the University of Žilina. She received the Ph.D. degree in applied mathematics in the field of functional differential equations in 2007, and the Habilitation degree in applied mathematics from the Slovak University of Technology, Bratislava, in 2017. Since 2000, she has been working as a University Teacher with the University of Žilina. Her scientific research

interests include functional differential equations, asymptotic properties of solutions, and dynamical systems.



**JAROSLAV HORNÁK** (Member, IEEE) was born in Klatovy, in 1989. He received the master's and Ph.D. degrees from the University of West Bohemia, Czech Republic, in 2014 and 2018, respectively. He completed a traineeship at P&G Rakona, Rakovník, Czech Republic, in 2016, and a practical internship at the Faculty of Electrical Engineering, University of Žilina, Žilina, Slovakia, in 2017. His research interests include research and development in the area of dielectric materials and diagnostics of their interactions with an electric field. He is currently a member of IEEE DEIS.



**PAVEL PROSR** (Member, IEEE) was born in Susice, Czech Republic, in 1979. He received the M.S. degree in electrical engineering and the Ph.D. degree from the University of West Bohemia, Pilsen, Czech Republic, in 2002 and 2005, respectively. In 2005, he joined the Department of Technologies and Measurement, University of West Bohemia, where he has worked as a Research Worker. Since 2012, he has been a Research and Development Specialist with the Regional Innovation Center for Electrical Engineering. He has published more than 170 research papers in journals and conference proceedings and has coauthored one monograph. His research interests include the study of the interaction between materials and the environment in electric systems, material diagnostics, and the application of structural analyses in electrical engineering.



**PAVEL TRNKA** (Senior Member, IEEE) received the M.Sc. and Ph.D. degrees from the University of West Bohemia, Czech Republic, in 2002 and 2005, respectively, and the Dr.hab. degree from the Faculty of Electrical Engineering, University of Žilina, Slovakia, in 2008. He was a student with the University of Applied Science, Fachhochschule, Regensburg, Germany, and worked with the Department of Research, Maschinenfabrik Reinhausen, Germany, from 2003 to 2004. From 2006 to 2007, he was a Postdoctoral Associate with the High Voltage Laboratory, Department of Electrical and Computer Engineering, Mississippi State University. He is currently a member of DEIS and the Executive Committee of the Czechoslovakia Section IEEE, and the Chairman of CDEE 2020.

• • •